BUTTERWORTH HEINEMANN

Polymer Vol. 36 No. 7, pp. 1341–1346, 1995

0032-3861/95/$10.00 + 0.00

Light-scattering studies of poly(*N*-isopropylacrylamide) in tetrahydrofuran and aqueous solution

Shuiqin Zhou, Shiyan Fan, Steve C. F. Au-yeung and Chi Wu*
Department of Chemistry, The Chinese University of Hong Kong, Shatin, New Territories, Hong Kong
(Received 14 July 1994; revised 8 September 1994)

Poly(*N*-isopropylacrylamide) (PNIPAM) was synthesized by free-radical polymerization. High resolution n.m.r. was used to confirm its chain composition and linear chain configuration. The solution properties of both unfractionated and fractionated PNIPAM samples in THF and water at 20°C were investigated by laser light scattering (LLS). Owing to its polyelectrolyte nature, it is extremely difficult, or nearly impossible, to obtain a set of narrowly distributed PNIPAM fractions with $M_w/M_n < 1.3$. Therefore, a scaling relationship between the translational diffusion coefficient (D) and the molar mass (M) has not yet been established. In this study, a combination of M_w from static LLS and the translational diffusion coefficient distribution ($G(D)$) from dynamic LLS results enabled us to establish D ($cm^2 s^{-1}$) $= 2.49 \times 10^{-4} M^{-0.540}$ for PNIPAM in THF at 20°C. Using this scaling relationship, we successfully calculated the molar mass distributions of a series of PNIPAM samples. For a given PNIPAM sample, the molar mass distributions obtained in different solvents are fairly comparable.

(Keywords: poly(*N*-isopropylacrylamide); laser light scattering; correlation between *D* and *M*)

INTRODUCTION

Poly(*N*-isopropylacrylamide) (PNIPAM) is a special kind of polyelectrolyte which contains both carbonyl and amide groups along its long and hydrophobic backbone chain. In aqueous media, slightly crosslinked PNIPAM forms a soft gel which can undergo a discontinuous, reversible volume phase transition in response to changes in temperature, salt content, solvent composition, pH and electric field[1]. This transition has substantial importance from medical, technological and scientific points of view[2]. There is a general description of this type of transition. However, the detailed mechanism is still not clear. Therefore, a better understanding of the PNIPAM molecular chain is a vital step towards the final explanation of this volume phase transition. As a promising material, PNIPAM has attracted much attention in both academic and industrial research[1]. Various methods have been used to study the solution behaviour of PNIPAM[3–7]. PNIPAM synthesized from a free-radical polymerization is normally very broadly distributed with respect to molar mass. It is extremely difficult, or nearly impossible, to fractionate such a broadly distributed PNIPAM sample into a set of narrowly distributed samples. Therefore, to our knowledge, the relationship between the translational diffusion coefficient (D) and the molar mass (M) has never been positively established. In viscosity measurements, the Mark–Houwink equation $[\eta] = k_\eta M^{\alpha_\eta}$ obtained in different research groups varies significantly[5–7], probably because of the use of a set of broadly distributed samples. Great efforts have been expended in the past[5,6] to fractionate a broadly distributed PNIPAM sample into a set of samples with a narrower polydispersity index (M_w/M_n) of ~ 1.3, which is still too broad to be used in a theoretical modelling treatment.

In this work, we have adopted a recently developed laser light scattering (LLS) data analysis procedure[8–12] involving a combination of the weight-average molar mass (M_w) from static LLS and the translational diffusion coefficient distribution ($G(D)$) from dynamic LLS to study a set of broadly distributed PNIPAM samples. By this procedure, we have established a scaling relationship of the type $D = k_D M^{-\alpha_D}$ which is directly related to the chain conformation of PNIPAM in solution.

EXPERIMENTAL

Preparation of samples

Poly(*N*-isopropylacrylamide) was synthesized by the following procedure. First, *N*-isopropylacrylamide (purchased from Eastman Kodak) monomer was recrystallized three times in a benzene/n-hexane mixture; then, the purified monomer (18 g) was dissolved in 150 ml benzene with 1 mol% of recrystallized azobisisobutyronitrile added as initiator; and finally, this solution was degassed through three cycles of freezing and thawing. Polymerization was carried out by stirring the final degassed solution in an oil bath at 56°C for 30 h under a positive nitrogen pressure. After polymerization, the solvent was removed by evaporation. The resulting crude solid was further dried and then dissolved in acetone. The polymer

* To whom correspondence should be addressed

was finally recovered by adding the acetone solution dropwise into n-hexane. Upon filtering and drying, a white fabric-like polymer was obtained with a yield of 75%. This PNIPAM was fractionated in a carefully dried acetone/n-hexane mixture at room temperature. Both the unfractionated and fractionated samples were used in this study. Tetrahydrofuran (THF, high performance liquid chromatography grade) purchased from Aldrich was used without further purification. The resistivity of the distilled deionized water used in this study was 18.3 MΩ cm.

N.m.r. analysis

^1H and ^{13}C n.m.r. measurements were carried out using a Bruker ARX-500 superconducting Fourier transform n.m.r. spectrometer operating at 500.13 and 125.76 MHz, respectively. One-dimensional ^1H and ^{13}C spectra were measured using 4 and 6 μs pulsewidths at 48 and 45° respectively. ^1H decoupling was executed using the WALTZ 16 pulse sequence. For one-dimensional nuclear Overhauser effect (n.O.e.) measurements the pulsewidth was 7.5 μs.

Homonuclear ^1H–^1H correlation spectroscopy (COSY) experiments were carried out using the standard COSY-45 sequence. For data treatment, a squared sine-bell window function was used with 0° shift. The second dimension was zero filled to 512k prior to Fourier transformation.

Heteronuclear ^1H–^{13}C COSY was carried out using the X–H COSY sequence with ^1H decoupling using the WALTZ 16 sequence. The ^{13}C pulsewidth (90°C) was 12 μs, whereas a sine-bell window function was used with SSB = 3 shift for data treatment.

Laser light scattering

A commercial LLS spectrometer (ALV-5000, Langan in Hessen, Germany) was used with a vertically polarized argon ion laser (coherent INNOVA 90, operated at 488 nm and 300 mW) as the light source. The details of LLS instrumentation and theories have been described elsewhere[13,14]. All LLS measurements were carried out at 20.0 ± 0.1°C. The specific refractive index increments (dn/dc) of PNIPAM in THF and in water at 20°C were determined using a novel and high precision differential refractometer[15]. The measured dn/dc values of PNIPAM at 20°C and 488 nm in THF and in water were 0.107 and 0.167 ml g^{-1}, respectively.

RESULTS AND DISCUSSION

In static light scattering, the angular dependence of the excess absolute time-averaged scattered intensity, known as the excess Rayleigh ratio ($R_{vv}(\theta)$), was measured. For dilute solutions, by measuring $R_{vv}(\theta)$ at a set of concentrations C and scattering angles θ, we could determine the weight-average molar mass M_w, the second virial coefficient A_2 and the root-mean-square z-average radius $\langle R_g^2\rangle_z^{1/2}$ from a Zimm plot[16]. The results are summarized in *Table 1*. For the unfractionated samples, the agreement between the M_w values obtained in THF and in water is rather satisfactory. The identical R_g and A_2 values of PNIPAM in THF and in water indicate that there is no significant difference in the interactions between PNIPAM and these solvents at 20°C. For fractions 2–4, the values of A_2 and R_g in THF are comparable with those in the literature[5] for similar molar masses. However, in comparison with the fractionated sample with a similar molar mass, the values of A_2 and R_g for the unfractionated sample are quite different, i.e. A_2 is negative and R_g is larger.

At first, we attributed this negative A_2 to a possible chain structure difference in the PNIPAM synthesized in our laboratory. High resolution ^1H and ^{13}C n.m.r. was used to clarify this point. The ^1H and ^{13}C n.m.r. spectra for the monomer were measured in $CDCl_3$. The complete proton assignments are summarized in *Table 2* according to the labelling scheme in *Figure 1a*. The chemical shift

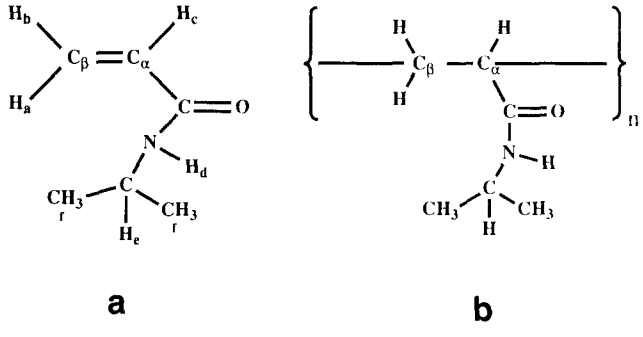

Figure 1 The labelling schemes of the monomer NIPAM (a) the polymer PNIPAM (b)

Table 2 Assignments of H species in the monomer NIPAM according to the labelling scheme in *Figure 1a*

δ(H, ppm)	Assignment	$^nJ_{ij}$(Hz) (multiplicity)
5.608	H_b	$^2J_{ba}$ = 1.47 (quartet) $^3J_{bc}$ = 16.96 (quartet)
6.260	H_a	$^3J_{bc}$ = 1.47 (quartet) $^3J_{ac}$ = 10.27 (quartet)
6.069	H_c	$^3J_{ca}$ = 10.27 (quartet) $^3J_{cb}$ = 16.96 (quartet)
5.619	H_d	$^3J_{de}$ = 7.56 (broad)
4.156	H_e	$^3J_{ed}$ = 7.56 (multiplet)
1.184	H_f	$^3J_{fe}$ = 6.30 (doublet)

Table 1 The light-scattering results of PNIPAM at 20°C

Sample	Solvent	M_w (g mol^{-1})	A_2 (mol ml g^{-2})	$\langle R_g^2\rangle_z^{1/2}$ (nm)	$10^8\langle D_0^0\rangle_z$ (cm^2 s^{-1})	$\langle R_h\rangle_z$ (nm)	$\frac{\langle R_g^2\rangle_z^{1/2}}{\langle R_h\rangle_z}$	$(M_w)_{calcd}$ (g mol^{-1})	$(M_w/M_n)_{calcd}$
Unfractionated	THF	2.45×10^6	-1×10^{-4}	103	6.78	65.2	1.58	2.47×10^6	7.54
Unfractionated	Water	2.40×10^6	-1×10^{-4}	103	3.27	65.3	1.57	2.40×10^6	6.75
Fraction 2	THF	3.97×10^6	1×10^{-4}	97	6.24	70.8	1.37	3.95×10^6	1.85
Fraction 3	THF	8.44×10^5	3×10^{-4}	50	13.7	32.3	1.56	8.44×10^5	2.17
Fraction 4	THF	8.61×10^4	6×10^{-4}	14	49.7	8.89	1.53	8.59×10^4	1.70

of the methyl protons was 1.184 (average between 1.190 and 1.177) ppm and the corresponding coupling constant with *N*-isopropyl proton was 6.30 Hz. Coupling between the amine proton (H_d) and the *N*-isopropyl proton (H_e) was also determined (7.56 Hz). The ^1H n.m.r. spectrum of the polymer was generally featureless. However, the AMX part of the spectrum from the terminal vinyl group in the monomer had disappeared, but very broad peaks in the methylene region were detected. This suggests that polymerization occurred through opening of the double bond in the monomer (see *Figure 1b*). This suggestion is supported by a comparison of the results obtained in the ^{13}C n.m.r. spectrum between the monomer and the polymer (*Figure 2*). In the ^{13}C n.m.r. spectrum of the monomer (*Figure 2a*), the peaks at 131 and 126 ppm are respectively assigned to C_α and C_β in the vinyl fragment. Both of these peaks are absent from the ^{13}C n.m.r. spectrum of the polymer, but two broad peaks are detected at 36 and 42.5 ppm in the methylene carbon region. The peak at 36 ppm is assigned to C_β, whereas that at 42.5 ppm is assigned to C_α, as shown in *Figure 1b*. Although the increase in molar mass and size because of polymer formation may lead to an increase in the correlation time, which may account for the extensive broadening in both the ^1H and the ^{13}C spectra, the presence of a distribution of backbone conformations in the polymer better accounts for the observed broadening of the ^{13}C n.m.r. peaks for C_α and C_β. No major changes were observed for the C=O and the isopropyl group. Finally, we think that this negative A_2 and larger R_g might be attributable to the broad distribution of the unfractionated sample, which contains some components with ultrahigh molar mass.

In dynamic light scattering, the normalized correlation function of the scattered electric field ($|g^{(1)}(t,\theta)|$) can be determined from a measured intensity–intensity time correlation function $G^{(2)}(t,\theta)$. For a polydisperse sample, $|g^{(1)}(t,\theta)|$ is related to $G(\Gamma)$ by

$$|g^{(1)}(t,\theta)| = \langle E(t,\theta)E^*(t,\theta)\rangle = \int_0^\infty G(\Gamma)e^{-\Gamma t}d\Gamma \quad (1)$$

where $G(\Gamma)$ is the normalized characteristic linewidth distribution. For finite q and C, the characteristic linewidth Γ can generally be expressed as[17,18]

$$\Gamma/q^2 = D_0^0(1+k_dC)(1+f\langle R_g^2\rangle q^2) \quad (2)$$

where k_d is the second virial diffusion coefficient and f is a dimensionless constant which depends on polydispersity, chain structure and solvent quality. Therefore, we can reduce $G(\Gamma)$ to the translational diffusion coefficient $G(D)$.

Figure 3 shows two typical translational diffusion coefficient distributions for the unfractionated PNIPAM sample in THF and in water at 20°C. For the sake of comparison, D has been scaled by the solvent viscosity (η). As expected, for a given PNIPAM sample, the distributions obtained in different solvents are very similar in shape and peak position. Both the distributions in *Figure 3* have a long tail in the large diffusion coefficient

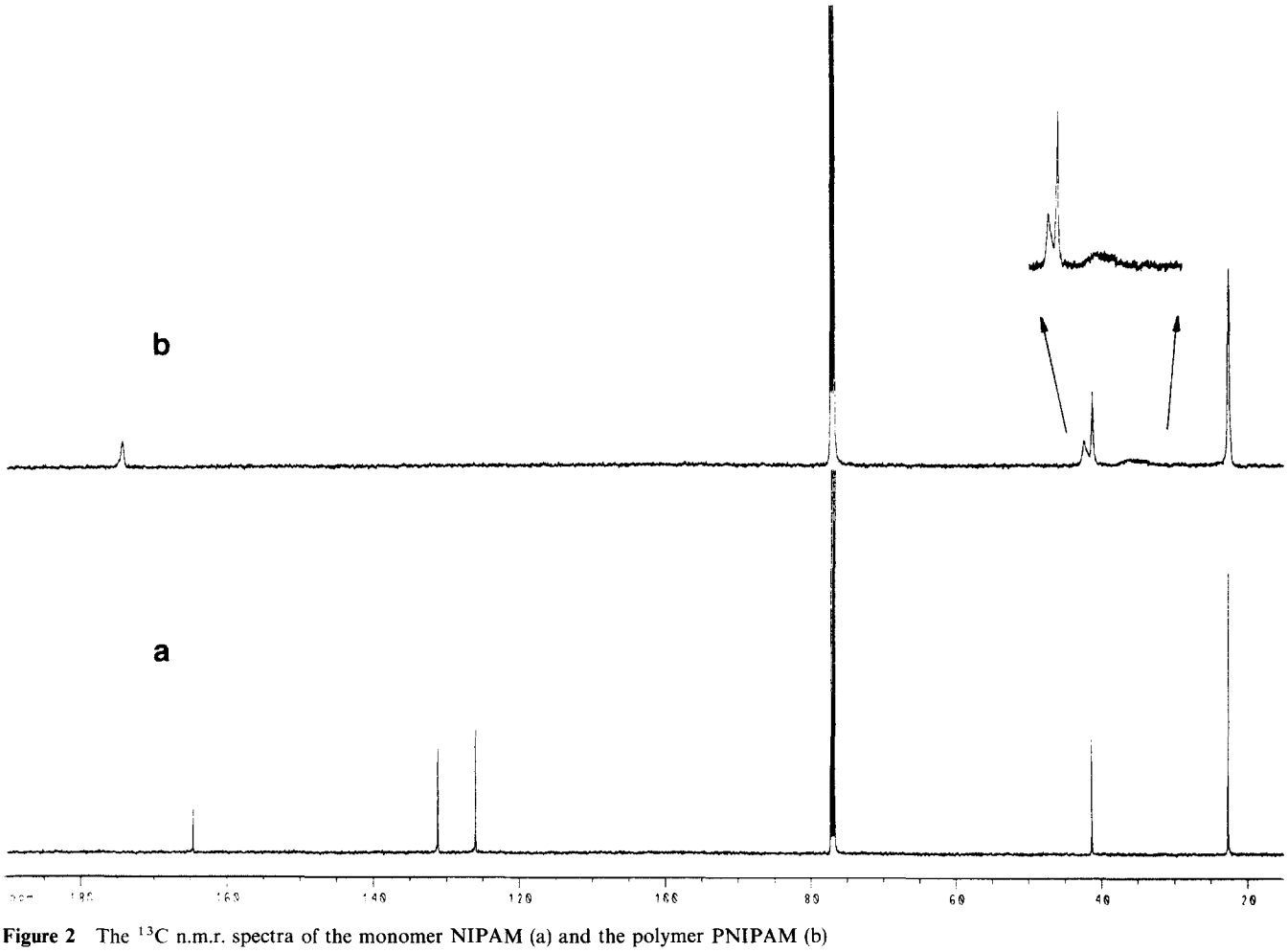

Figure 2 The ^{13}C n.m.r. spectra of the monomer NIPAM (a) and the polymer PNIPAM (b)

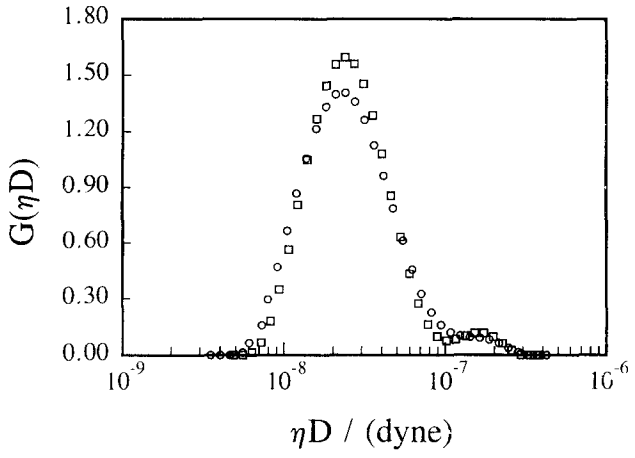

Figure 3 Translational diffusion coefficient distributions of the unfractionated PNIPAM sample measured in THF (□) and in water (○) as $c\to 0$ and $\theta\to 0$ at 20°C, where D has been scaled by the solvent viscosity (η) for the sake of comparison

and which corresponds to low molar mass PNIPAM. This long tail indicates that the unfractionated PNIPAM sample has a very broad molar mass distribution. The distributions of the three fractionated PNIPAM samples are narrower than those in *Figure 3*, but still too broad to be used in a theoretical modelling treatment.

On the basis of equation (2), we can get $\langle D_0^0\rangle_z$ from a dynamic Zimm plot as $q\to 0$ and $c\to 0$. Furthermore, the average hydrodynamic radius $\langle R_h\rangle_z$ can be calculated by replacing D with $\langle D_0^0\rangle_z$ in the Stokes–Einstein equation $R_h = k_B T/6\pi\eta D$, where k_B, η and T are the Boltzmann constant, the solvent viscosity and absolute temperature, respectively. The values of $\langle D_0^0\rangle_z$, $\langle R_h\rangle_z$ and $\langle R_g^2\rangle_z^{1/2}/\langle R_h\rangle_z$ are listed in *Table 1*. It can be seen that the value of $\langle R_g^2\rangle_z^{1/2}/\langle R_h\rangle_z$ for the unfractionated PNIPAM sample in THF is similar to that in water. We can conclude that the solvent qualities of THF and water are similar for the broadly distributed unfractionated PNIPAM sample at 20°C. The values of $\langle R_g^2\rangle_z^{1/2}/\langle R_h\rangle_z$ for both the unfractionated and fractionated PNIPAM samples in THF are larger than the values in the literature[5]. It should be noted that Kubota *et al.*[5] made a mistake in converting D to R_h in which they mistook $\eta_{THF}^{20°C}$ (0.486) for $\eta_{toluene}^{25°C}$ (0.551). After recalculating $\langle R_h\rangle_z$ with the right viscosity, the value of $\langle R_g^2\rangle_z^{1/2}/\langle R_h\rangle_z$ for Kubota *et al.*[5] would be 1.23–1.25, which is too low for a linear polymer chain in a good solvent. In addition, this value is in stark contrast to the α_η value of 0.65 in the Mark–Houwink relationship of PNIPAM in THF at 27°C[6]. In comparison, the values of $\langle R_g^2\rangle_z^{1/2}/\langle R_h\rangle_z$ ($\sim$1.55) obtained in this work are more reasonable, showing that the PNIPAM chain has a coil conformation in THF at 20°C.

Besides the Mark–Houwink equation, the scaling relationship between D and M, i.e. $D = k_D M^{-\alpha_D}$, is often used nowadays to characterize polymer chains in solution, where α_D is directly linked to the chain conformation. This linkage has been theoretically predicted and experimentally proven. Normally, α_D can be obtained by measuring both D and M for a set of narrowly distributed standards. Unfortunately, owing to its polyelectrolyte nature, it is extremely difficult, or nearly impossible, to get a set of such narrowly distributed PNIPAM standards. Therefore, we have to solve this problem in a different way.

On the one hand, from static light scattering when $c\to 0$ and $\theta\to 0$ we have

$$\int_0^\infty F_w(M) M\, dM \propto I \tag{3}$$

where $F_w(M)$ is a weight-average molar mass distribution. On the other hand, on the basis of equation (1) as $t\to 0$ we have

$$[g^{(1)}(t,\theta)]_{t\to 0} = \int_0^\infty G(\Gamma)\, d\Gamma \propto \int_0^\infty G(D)\, dD \propto I \tag{4}$$

Combination of equations (3) and (4) leads to

$$\int_0^\infty F_w(M) M\, dM \propto \int_0^\infty G(D)\, dD \tag{5}$$

which can be further written as

$$\int_0^\infty F_w(M) M^2\, d(\ln M) \propto \int_0^\infty G(D) D\, d(\ln D) \tag{6}$$

where $d(\ln M)\propto d(\ln D)$ according to $D = k_D M^{-\alpha_D}$. After comparing both sides of equation (6), it is not too difficult to find that

$$F_w(M) \propto \frac{G(D)D}{M^2} \propto G(D) D^{1+2/\alpha_D} \tag{7}$$

All proportionality constants have been omitted from equations (3)–(7) since they are irrelevant to a given distribution. By definition

$$(M_w)_{calcd} = \frac{\int_0^\infty F_w(M) M\, dM}{\int_0^\infty F_w(M)\, dM} = \frac{k_D^{1/\alpha_D}\int_0^\infty G(D)\, dD}{\int_0^\infty G(D) D^{1/\alpha_D}\, dD} \tag{8}$$

where we have used $dD \propto M^{-(\alpha_D+1)} dM$ on the basis of $D = k_D M^{-\alpha_D}$.

Figure 4 shows a double-logarithmic plot of $\langle D_0^0\rangle_z$ *versus* M_w for PNIPAM in THF at 20°C. The solid line represents a least-squares fitting of $\langle D_0^0\rangle_z = \langle k_D\rangle M_w^{-\langle\alpha_D\rangle}$ with $\langle k_D\rangle = (2.86\pm 0.10)\times 10^{-4}$ and $\langle\alpha_D\rangle = 0.56\pm 0.02$, where '$\langle\ \rangle$' means that the values are obtained from $\langle D_0^0\rangle_z$

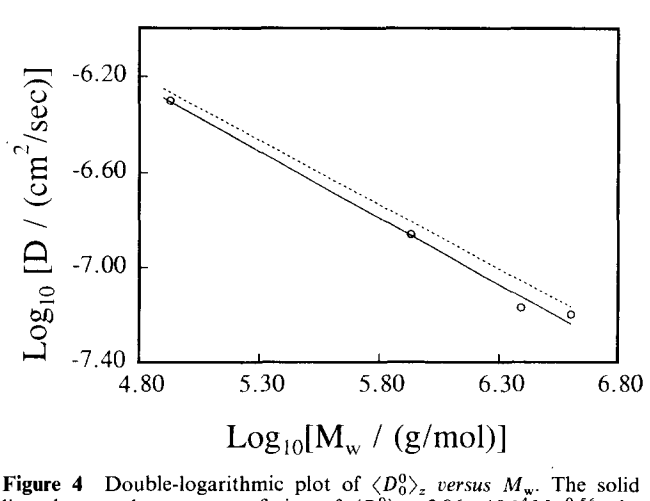

Figure 4 Double-logarithmic plot of $\langle D_0^0\rangle_z$ *versus* M_w. The solid line shows a least-squares fitting of $\langle D_0^0\rangle_z = 2.86\times 10^{-4} M_w^{-0.56}$; the dashed line represents a correlation between D and M, i.e. $D = 2.49\times 10^{-4} M^{-0.540}$, instead of between $\langle D_0^0\rangle_z$ and M_w

and M_w instead of D and M. At first, we tried to replace k_D with $\langle k_D \rangle$ and α_D with $\langle \alpha_D \rangle$ in equation (8) to calculate $(M_w)_{calcd}$ from $G(D)$, but we found that such $(M_w)_{calcd}$ values were much smaller than the measured M_w values from static LLS. It is known in general that $\langle k_D \rangle$ and $\langle \alpha_D \rangle$ obtained from a set of broadly distributed samples are usually different from k_D and α_D, which forced us to use a recently developed method to obtain k_D and α_D, instead of $\langle k_D \rangle$ and $\langle \alpha_D \rangle$, from two or more broadly distributed samples[8-12]. For the convenience of this discussion, this method is outlined in the following.

For N-number samples, we have N-number M_w values from static LLS and N-number $G(D)$ values from dynamic LLS denoted as $M_{w,i}$ and $G_i(D)$, where $i = 1, 2, \ldots, N$. By assuming a pair of k_D and α_D and using equation (8), we are able to calculate the N-number $(M_w)_{calcd}$, denoted as $(M_{w,i})_{calcd}$. The ratio of $(M_{w,i})_{calcd}/(M_{w,j})_{calcd}$ is

$$\frac{(M_{w,i})_{calcd}}{(M_{w,j})_{calcd}} = \frac{\left[\int_0^\infty G_i(D)\,dD\right]\left[\int_0^\infty G_j(D)D^{1/\alpha_D}\,dD\right]}{\left[\int_0^\infty G_j(D)\,dD\right]\left[\int_0^\infty G_i(D)D^{1/\alpha_D}\,dD\right]} \quad (9)$$

where k_D has been eliminated. In principle, $(M_{w,i})_{calcd}$ should equal $M_{w,i}$ if α_D and k_D are properly chosen, and then the difference between $M_{w,i}/M_{w,j}$ and $(M_{w,i})_{calcd}/(M_{w,j})_{calcd}$ should reach a minimum. On the basis of the above discussion, two error functions are defined as

$$ERROR(\alpha_D) = \sum_{i=1,j=1}^{N} \left[\frac{M_{w,i}}{M_{w,j}} - \frac{(M_{w,i})_{calcd}}{(M_{w,j})_{calcd}}\right]^2 \quad (10)$$

and

$$ERROR(k_D) = \sum_{i=1}^{N} [M_{w,i} - (M_{w,i})_{calcd}]^2 \quad (11)$$

It is clear that this procedure is an M_w-constrained analysis. First, by iteration for α_D, we can find a proper α_D to minimize $ERROR(\alpha_D)$; and then, with this α_D, we can find k_D by iteration to minimize $ERROR(k_D)$. In this way, we are able to obtain k_D and α_D with only a set of broadly distributed samples.

On the basis of equation (10), we found a minimum value of $ERROR(\alpha_D)$ at $\alpha_D = 0.540$ by iteration for α_D. At this α_D value, the measured results from static and dynamic LLS, i.e. M_w and $G(D)$, are well matched. *Figure 5* shows typical plots of $ERROR(k_D)$ *versus* k_D for different values of α_D. It can be seen that there exists a minimum $ERROR(k_D)$ for each given α_D and there exists an overall minimum at $\alpha_D = 0.540$ and $k_D = 2.49 \times 10^{-4}$. This pair of α_D and k_D defines a correlation, or scaling relationship, between D and M, instead of between $\langle D_0^0 \rangle_z$ and M_w, which is also drawn in *Figure 4* (dashed line). After getting k_D and α_D, we can convert $G(D)$ to $F_w(M)$ according to equation (7).

The $F_w(M)$ values of unfractionated and fractionated PNIPAM samples were calculated from the $G(D)$ values by using $D = 2.49 \times 10^{-4} M^{0.540}$. The values of the polydispersity index M_w/M_n calculated from these $F_w(M)$ values are presented in *Table 1*. It is expected that the $F_w(M)$ of the unfractionated sample will be much broader than that of any fractionated sample. In addition, the unfractionated sample has a bimodal distribution. At this moment, we have no explanation for the connection between this bimodal distribution and the polymerization kinetics.

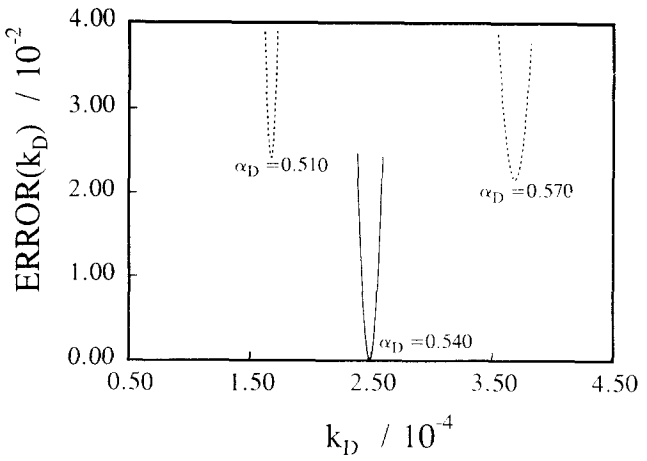

Figure 5 Typical plots of $ERROR(k_D)$ *versus* k_D for different values of α_D. The overall minimum value of $ERROR(k_D)$ corresponds to $\alpha_D = 0.540$ and $k_D = 2.49 \times 10^{-4}$

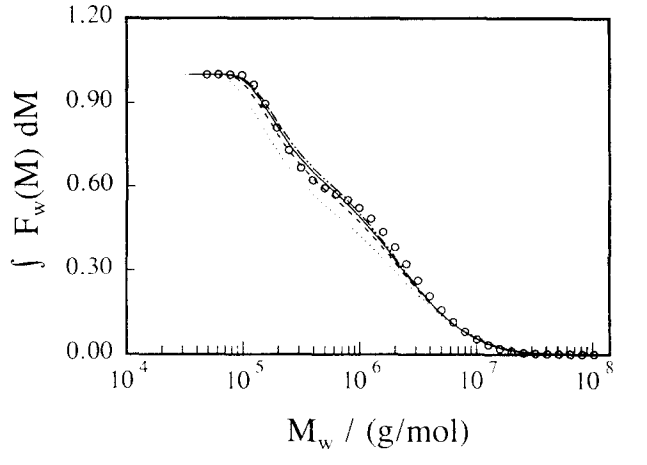

Figure 6 Comparison of the cumulative molar mass distributions of the unfractionated PNIPAM sample obtained in water and THF. For water, four different α_D values were used: (·····) $\alpha_D = 0.50$; (- - -) $\alpha_D = 0.54$; (——) $\alpha_D = 0.55$; (— - —) $\alpha_D = 0.56$. For THF, $\alpha_D = 0.54$ (○) was used

The relationship between D and M for PNIPAM in aqueous solution is even more controversial. The first report of the Mark–Houwink coefficient α_η for PNIPAM in aqueous solution at 20°C was 0.93 by Chiantore *et al.*[7] where a number of unfractionated samples were used. This α_η value implies that the PNIPAM chain in water is an extended coil at 20°C. Kubota *et al.*[5] and Fujishige[6] determined the α_η value (~ 0.50) of PNIPAM in water at 20°C by using a set of fractionated samples with a narrower molar mass distribution ($M_w/M_n \approx 1.3$). According to Flory[19], α_D and α_η are related by $\alpha_D = (1 + \alpha_\eta)/3$. If their[5,6] α_η is correct, the value of α_D should be 0.50, which means that water is a θ solvent for PNIPAM at 20°C. However, according to their A_2 values, the θ temperature is 30.59°C, which is reasonable since it is near the lower critical solution temperature of PNIPAM in equeous solution. Therefore, there is a contradiction between their α_η value (~ 0.50) and their positive A_2 values at 20°C. In order to find the proper α_D and k_D of PNIPAM in aqueous solution at 20°C, we have utilized the following fact: for a given PNIPAM sample, its molar mass distribution

should be independent of the type of solvent used in its characterization, i.e. $F_w(M)$ values obtained from $G(D)$ values in *Figure 3* should be the same.

Figure 6 shows five cumulative molar mass distributions calculated from the $G(D)$ values in *Figure 3*. For PNIPAM in THF, we have used the previously determined scaling relationship $D = 2.49 \times 10^{-4} M^{-0.540}$ to convert $G(D)$ to $F_w(M)$. For PNIPAM in water, we have tried four different values of α_D. *Figure 6* shows that if $\alpha_D = 0.50$, the difference between the molar mass distributions obtained in water and in THF is large. In contrast, if $\alpha_D = 0.54$–0.56, the difference is less significant. After considering all the experimental uncertainties, we conclude that the proper values of α_D and k_D for PNIPAM in water at 20°C should be 0.55 ± 0.01 and $(1.36 \pm 0.10) \times 10^{-4}$, respectively. With this pair of α_D and k_D, we finally converted the $G(D)$ of the unfractionated PNIPAM in aqueous solution at 20°C in *Figure 3* into $F_w(M)$. The calculated value of M_w/M_n is listed in *Table 1*, and it agrees well with the value obtained from THF solution. This α_D value of 0.55 ± 0.01 is also very close to the value of 0.56 which can be derived from the data in the literature[5].

CONCLUSIONS

The solution properties of PNIPAM in both THF and water at 20°C have been studied by using a combination of static and dynamic LLS. The scaling relationships between the translational diffusion coefficient (D) and the molar mass (M), instead of $\langle D \rangle_z$ and M_w, of PNIPAM in both THF and water at 20°C have been established from a set of broadly distributed samples, wherein we have used the following facts: (1) the weight-average molar mass (M_w) measured from static LLS should be the same as that calculated from the translational diffusion coefficient distribution ($G(D)$) in dynamic LLS; and (2) for a given PNIPAM sample, the molar mass distribution should be independent of the solvent used in the LLS characterization. From the α_D and A_2 values of PNIPAM in THF and water at 20°C, we are confident in concluding that both THF and water are fairly good solvents for PNIPAM at 20°C and the PNIPAM chain in both THF and water at 20°C has a flexible coil conformation.

ACKNOWLEDGEMENTS

We gratefully acknowledge the financial support of this work by an Earmarked Research Grant (221600140) from the Research Grants Council of the Hong Kong Government.

REFERENCES

1 Schild, H. G. *Prog. Polym. Sci.* 1992, **17**, 163 and references therein
2 Tanaka, T. *ACS Symp. Ser.* 1992, **480**, 1 and references therein
3 Fujishige, S., Kubota, K. and Ando, I. *J. Phys. Chem.* 1989, **93**, 3311
4 Kubota, K., Fujishige, S. and Ando, I. *J. Phys. Chem.* 1990, **94**, 5154
5 Kubota, K., Fujishige, S. and Ando, I. *Polym. J.* 1990, **22**, 15
6 Fujishige, S. *Polym. J.* 1987, **19**, 297
7 Chiantore, O., Guaita, M. and Trossarelli, L. *Makromol. Chem.* 1979, **180**, 969
8 Wu, C., Zuo, J. and Chu, B. *Macromolecules* 1989, **22**, 633
9 Wu, C. and Lilge, D. *J. Appl. Polym. Sci.* 1993, **50**, 1753
10 Wu, C. *Macromolecules* 1993, **26**, 3821
11 Wu, C. *J. Polym. Sci., Polym. Phys. Edn* 1994, **32**, 803
12 Wu, C., Zhou, S. Q. and Wang, W. *Biopolymers* in press
13 Chu, B. 'Laser Light Scattering', Academic Press, New York, 1974
14 Pecora, R. 'Dynamic Light Scattering', Plenum Press, New York, 1976
15 Wu, C. and Xia, K. Q. *Rev. Sci. Instrum.* 1994, **65**, 587
16 Zimm, B. H. *J. Chem. Phys.* 1948, **16**, 1099
17 Stockmayer, W. H. and Schmidt, M. *Pure Appl. Chem.* 1982, **54**, 407
18 Stockmayer, W. H. and Schmidt, M. *Macromolecules* 1984, **17**, 509
19 Flory, P. J. 'Principles of Polymer Chemistry', Cornell University Press, Ithaca, NY, 1953